

# Briefing Space Weather

2022/06/27

## 1 Sun

### 1.1 Responsible: José Cecatto

06/20 – No flare (M/X); Fast wind stream ( $\leq 650$  km/s); 2 CME c.h.c. toward the Earth;  
06/21 – No flare (M/X); Fast wind stream ( $\leq 550$  km/s); 5 CME c.h.c. toward the Earth;  
06/22 – No flare (M/X); Fast wind stream ( $\leq 500$  km/s); 6 CME c.h.c. toward the Earth;  
06/23 – No flare (M/X); Fast wind stream ( $\leq 500$  km/s); 5 CME c.h.c. toward the Earth;  
06/24 – No flare (M/X); Fast wind stream ( $\leq 450$  km/s); 4 CME c.h.c. toward the Earth;  
06/25 – No flare (M/X); Fast wind stream ( $\leq 500$  km/s); 2 CME c.h.c. toward the Earth;  
06/26 – No flare (M/X); Fast wind stream ( $\leq 700$  km/s); 8 CME c.h.c. toward the Earth;  
06/27 – No flare (M/X); Fast wind stream ( $\leq 650$  km/s); No CME toward the Earth;  
Prev.: Fast wind stream up to June 28; for the next 2 days low (10% M, 1% X) probability of M / X flares; also, occasionally other CME can present component toward the Earth.  
c.h.c. – can have a component; \* partial halo; \*\* halo

## 2 Sun

### 2.1 Responsible: Douglas Silva

- WSA-ENLIL (Prediction for CME 2022-06-19T21:53Z)
  - The simulation results indicate that the flank of CME will reach the DSCOVR mission between 05:00Z and 19:30Z on 22nd June 2022.
- WSA-ENLIL (CME 2022-06-21T00:48Z )
  - The simulation results indicate that the flank of CME will reach the DSCOVR mission between 2022-06-24T05:00Z and 2022-06-24T19:00Z.

Buracos coronais (SPoCA : Spatial Possibilistic Clustering Algorithm):

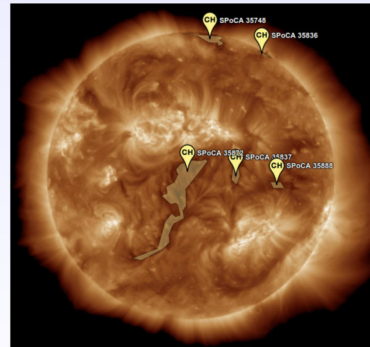
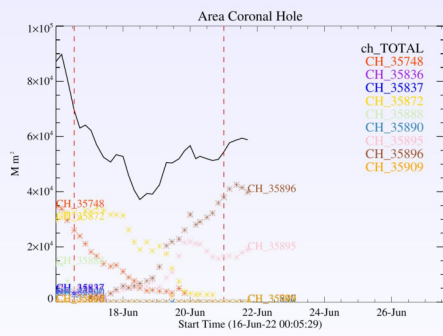
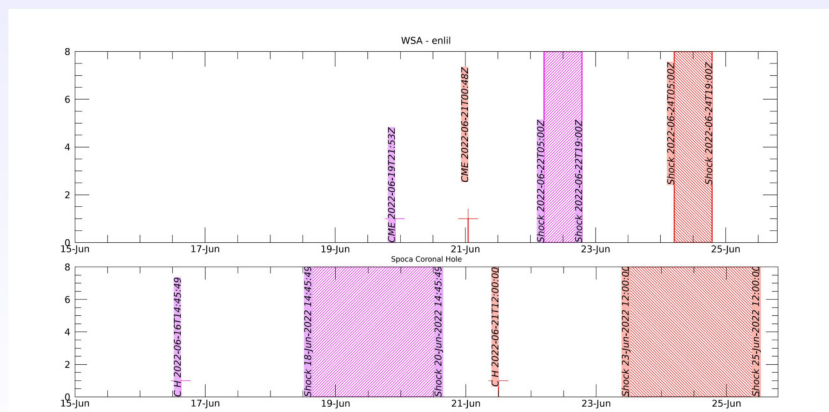


Figura: A linha em preto mostra o resultado da soma das areas para cada intervalo da detecção realizado pelo SPOCA entre os dias 16 de junho e 22 de junho de 2022

Sobre a imagem em 193 Å do Sol estão destacados os Buracos coronais observados pelo SPOCA por volta das 14:45 UT do dia 16 de junho de 2022.



WSA - ENLIL SPOCA

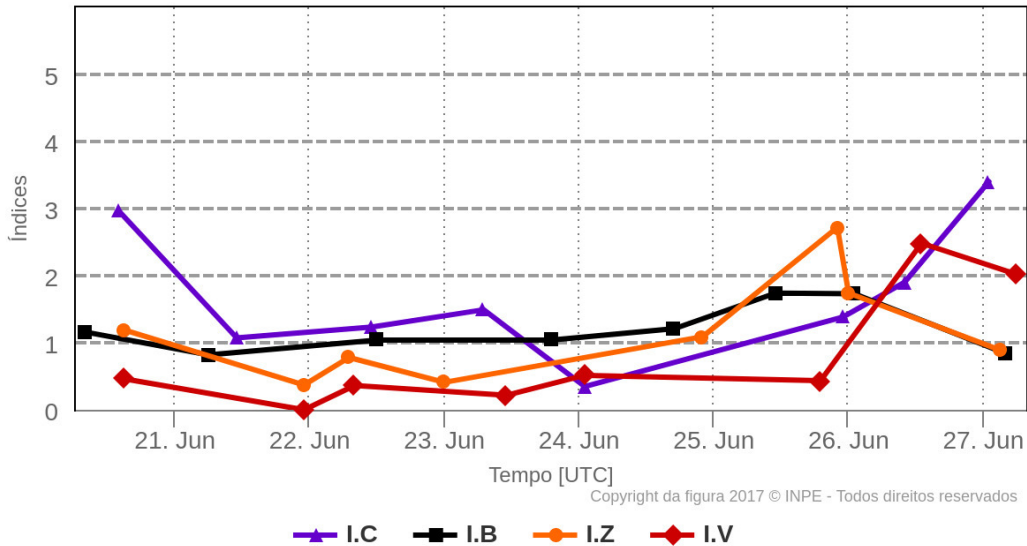


## 3 Interplanetary Medium

### 3.1 Responsible: Paulo Jauer

#### Resumo dos índices do meio interplanetário

Máximos diários - mais recentes entre 20 Jun, 2022 e 27 Jun, 2022



- The interplanetary medium region in the last week showed a low/moderate level of plasma perturbations due to the possible interaction of CIR and HSS-like structures identified by the DISCOVER satellite in the interplanetary medium.
- The modulus of the interplanetary magnetic field component showed 1 maximum peak on June 25 at 11:30 from  $\sim 13.2$  nT.
- The BxBy components showed variations in the analyzed period, both remaining oscillating within the  $[+11, -11]$  nT interval, with the presence of a sector change on June 21 at 14:30 UT. The component of the bz field showed fluctuations oscillating mostly in the  $[+5, -5]$  nT interval.
- The bz component presented a change of direction on June 24 at 15:30 due to the interaction of a CIR, whose peak value of the IMF Bz south recorded was  $\sim -10$  nT.
- The solar wind density showed a maximum peak on June 27 at 00:30 of  $46.8 p/cm^3$ , it also presented other peaks that oscillated below  $22 p/cm^3$ . The density remained oscillating on average below  $12 p/cm^3$  in the rest of the period.
- The speed of the solar wind had fluctuated and remained above 400 km/s throughout the period. Presenting maximum peak of 620 and 663 km/s on June 20-26 at 15:30 and 13:30 respectively.
- The magnetopause position was oscillating on average below the equilibrium position. On June 27 at 01:30, it presented a maximum compression of 6.9 Re. She had two other compressions on June 20-26 at 2:30 pm and 10:30 UT of 7.38 and 8.3 Re respectively.

## 4 Radiation Belts

### 4.1 Responsible: Ligia Alves da Silva

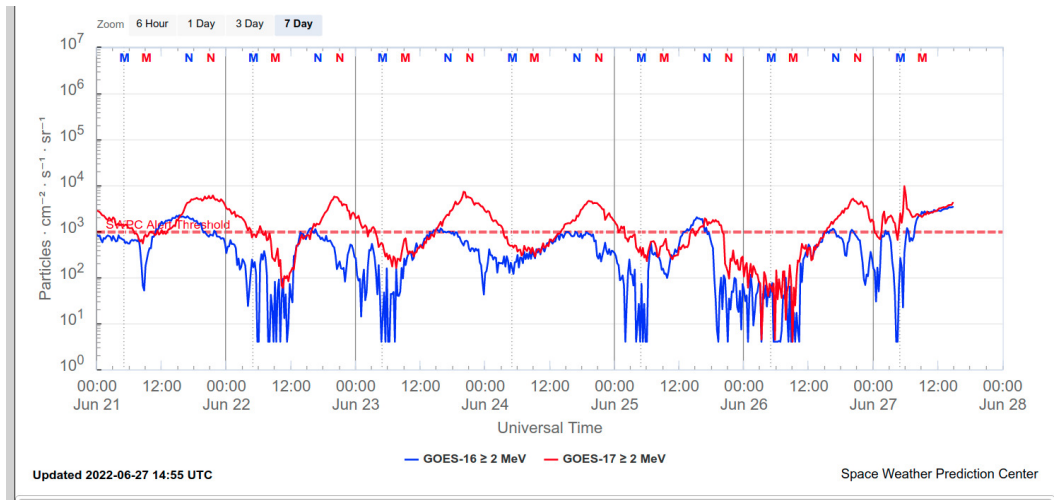


Figura 1: High-energy electron flux ( $\geq 2\text{MeV}$ ) obtained from GOES-16 and GOES-17 satellite. Source: <https://www.swpc.noaa.gov/products/goes-electron-flux>.

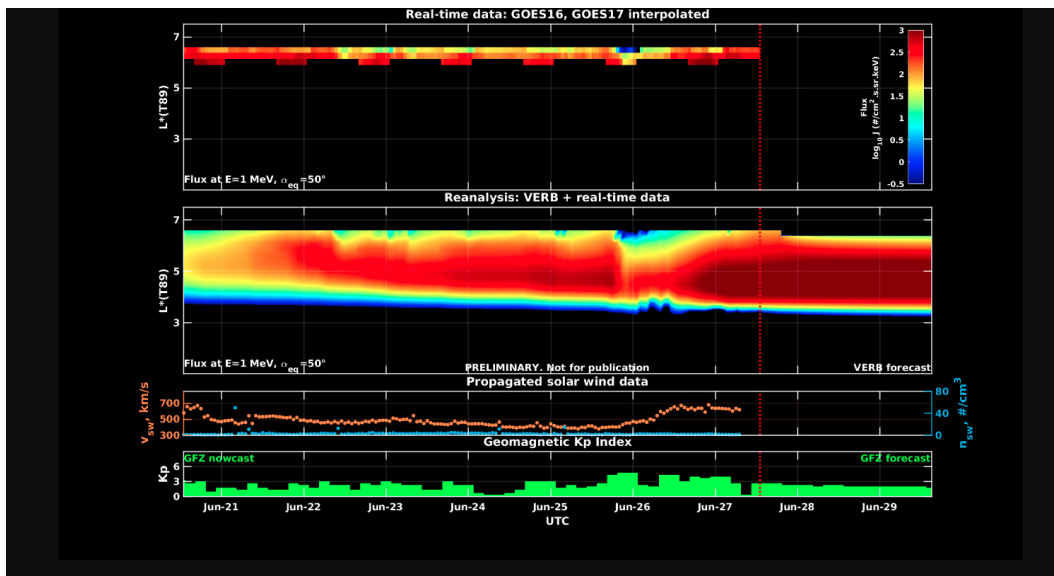


Figura 2: high-energy electron flux data (real-time and interpolated) obtained from ARASE, GOES-16, GOES-17 satellites. Reanalysis's data from VERB code and interpolated electron flux. Solar wind velocity and proton density data from ACE satellite. Source: <https://rbm.epss.ucla.edu/realtime-forecas>.

High-energy electron flux ( $> 2\text{ MeV}$ ) in the outer boundary of the outer radiation belt obtained from geostationary satellite data GOES-16 and GOES-17 (Figure 1) oscillates between  $10^2$  and  $10^4$  particles/( $\text{cm}^2\text{ssr}$ ) for almost the entire analyzed period. Four electron flux decrease were observed, but only the dropout observed the end of June 25th reached more than two orders of magnitude.

The GOES-16, GOES-17, and Arase satellite data are analyzed and interpolated to observe the high-energy electron flux variability (1 MeV) in the outer radiation belt (Figure 2). Additionally, the VERB code rebuilds this electron considering the Ultra Low Frequency (ULF) waves' radial diffusion. The simulation (VERB code) shows that the dropout observed at the end of June 15th reached L-shell  $> 3.5$ . This was followed by an electron flux increase from the end of June 26th. The electron flux variabilities

occurred concomitantly with arrival of solar wind structures in the magnetosphere and the ULF wave activities.

## 5 ULF waves

### 5.1 Responsible: Graziela B. D. Silva

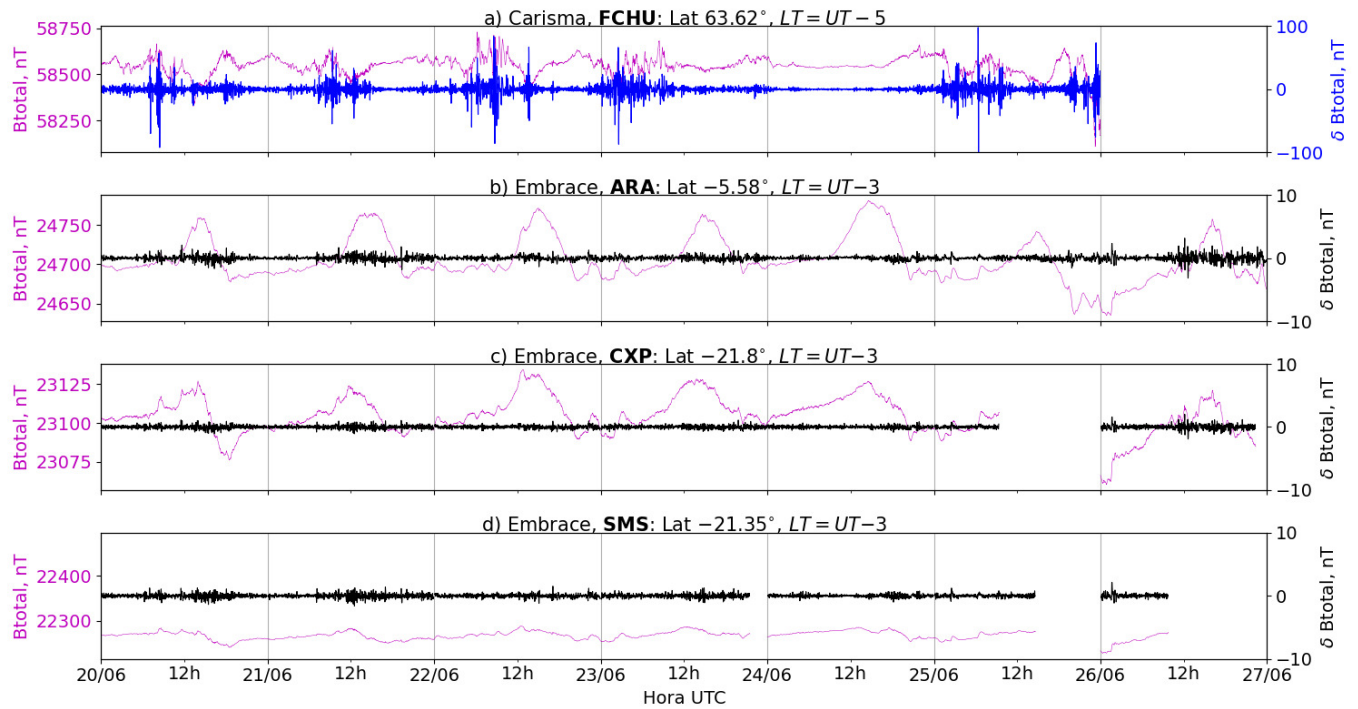


Figura 3: a) Timeseries of the geomagnetic field total component measured at FCHU station (Fort Churchill) of the CARISMA magnetometer network in magenta, along with the associated perturbation in the Pc5 band shown in blue. b-d) timeseries of the geomagnetic field total component measured at stations ARA (Araguatins), CXP (Cachoeira Paulista) and SMS (São Martinho da Serra) of the EMBRACE network in magenta, along with the Pc5 perturbation in blue.

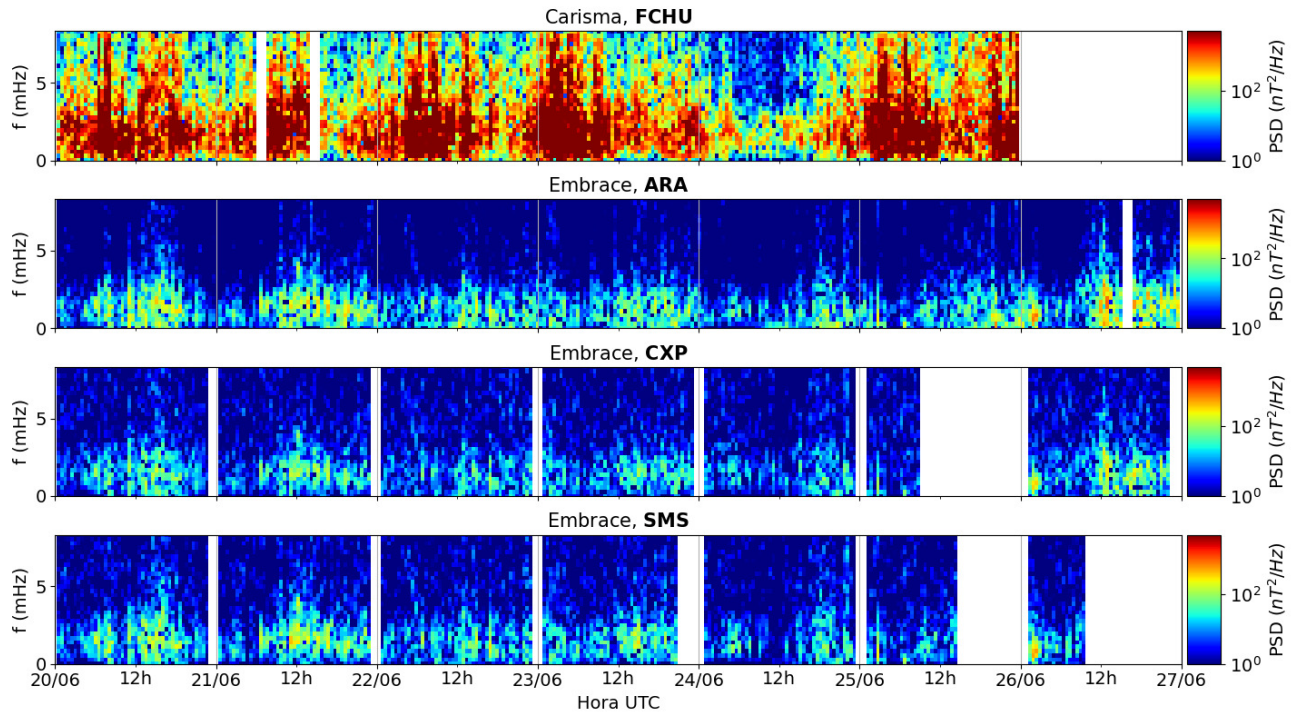


Figura 4: a-d) Time evolution of the power spectral density obtained from the filtered timeseries of the geomagnetic field total component ( $\delta B_{total}$ ) for a) the high latitude station (FCHU-CARISMA), and b-d) for the low latitude stations of EMBRACE (ARA, CXP, SMS).

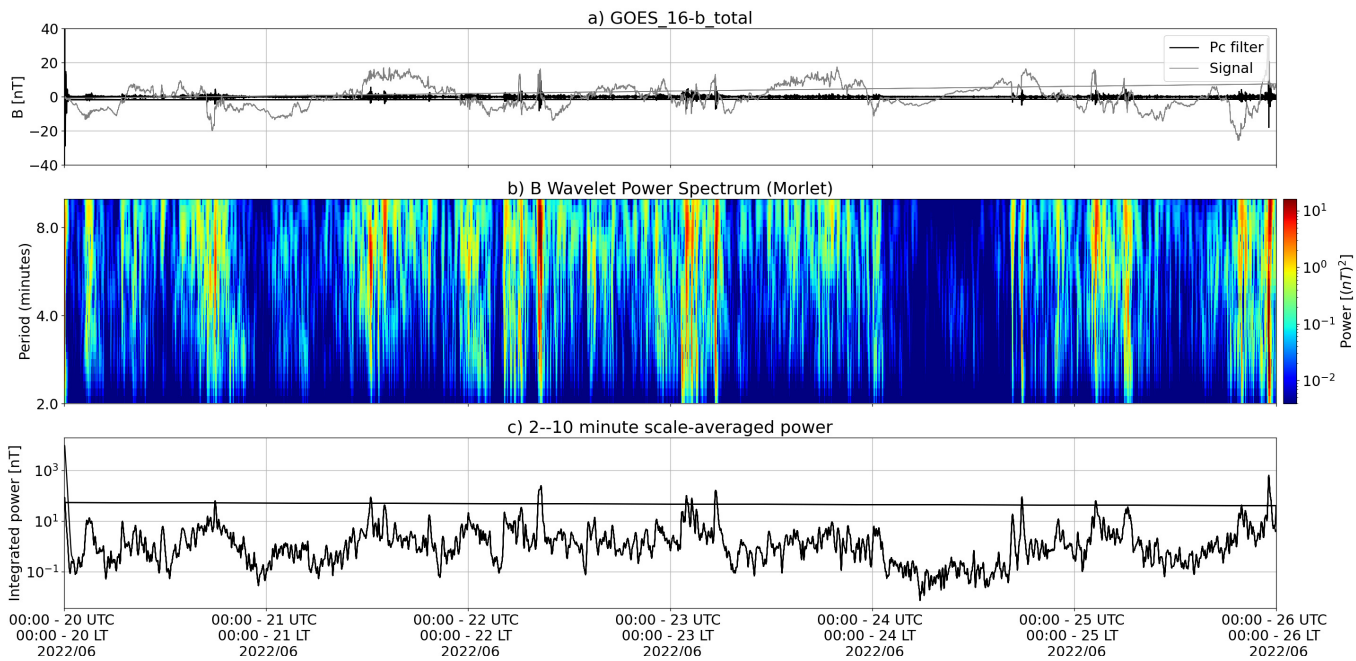


Figura 5: a) Timeseries of the geomagnetic field total component measured by GOES 16, together with the Pc5 fluctuation in black. b) Wavelet power spectrum of the filtered timeseries. c) Average ULF power in the period range from 2 to 10 minutes.

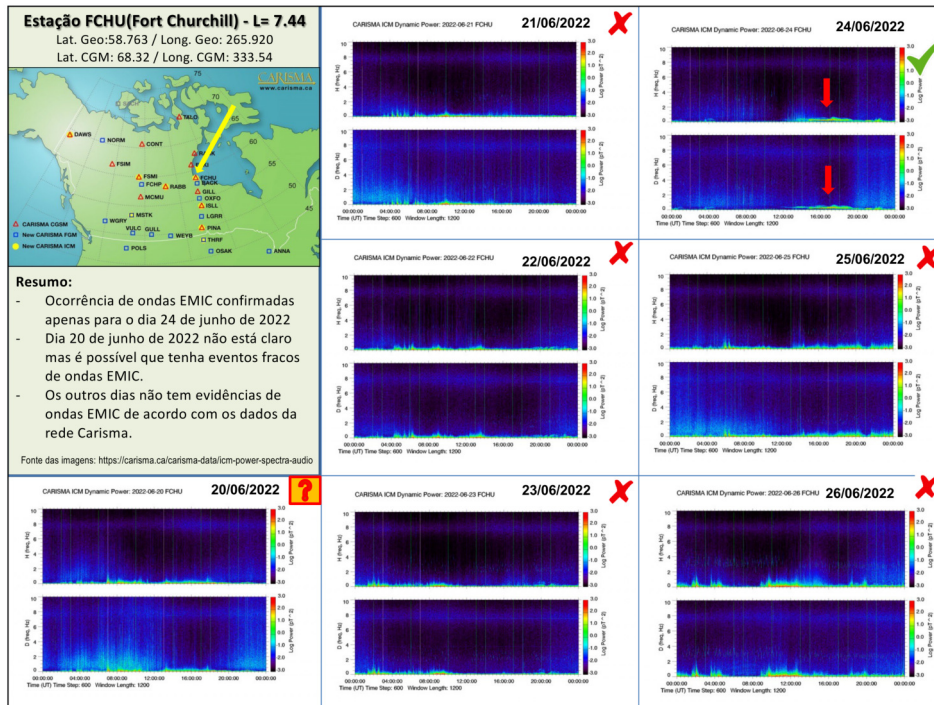
- There was moderate to intense and continuous activity of Pc5 ULF waves over the week measured by GOES-16 at the geosynchronous orbit, except on 24/june. The reported wave activity was associated to the passing of an ICME on 22/june and a CIR (corotating interaction region) on

26/june. between 06/june and 07/june, as measured by GOES 16 at geosynchronous orbit ( $L \sim 6.6$ ). The wave activity was associated with the arrival of an ICME (interplanetary coronal mass ejection) on 06/june.

- For the ground-based stations, an intense activity of ULF waves was registered at Fort Churchill (FCHU/high latitude) up to 25/june, while a small activity was present on 24/june, in accordance with results obtained by GOES-16.
- There is no available data for analysis of 26/june.
- At the Embrace stations over the Brazilian equatorial region, there was moderate to intense or weak activity of ULF waves over the week, even on 24/june (the least disturbed day of the week.)
- Comparing the spectral power results between signals recorded in Vassouras and Cahoeira Paulista, it was noticed that the ULF wave signals in VSS are generally weaker, indicating a certain level of damping of the Pc5 waves at this station.

## 6 EMIC waves

### 6.1 Responsible: Claudia Medeiros



## 7 Geomagnetic activity

### 7.1 Responsible: Lívia Alves

In the week of 21-27 June, the following events related to geomagnetic activity stand out:

- The data from the Embrace magnetometer network showed instabilities throughout the period, with emphasis on Jun 25-27 - The magnetometers of the Embrace network recorded a drop followed by an enhancement in the H component.
- The geomagnetic activity was unstable throughout the period, the AE index was unsettled in the period, AE index reached 1000 nT. The Dst index reached -50 nT. The highest Kp of the week was 4<sup>o</sup>.
- The geomagnetic field measured at the GOES orbit shows instabilities on 22 and 25-June.

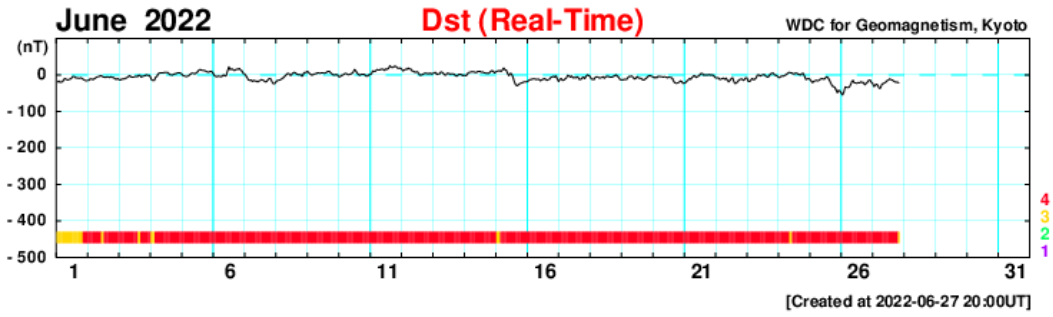


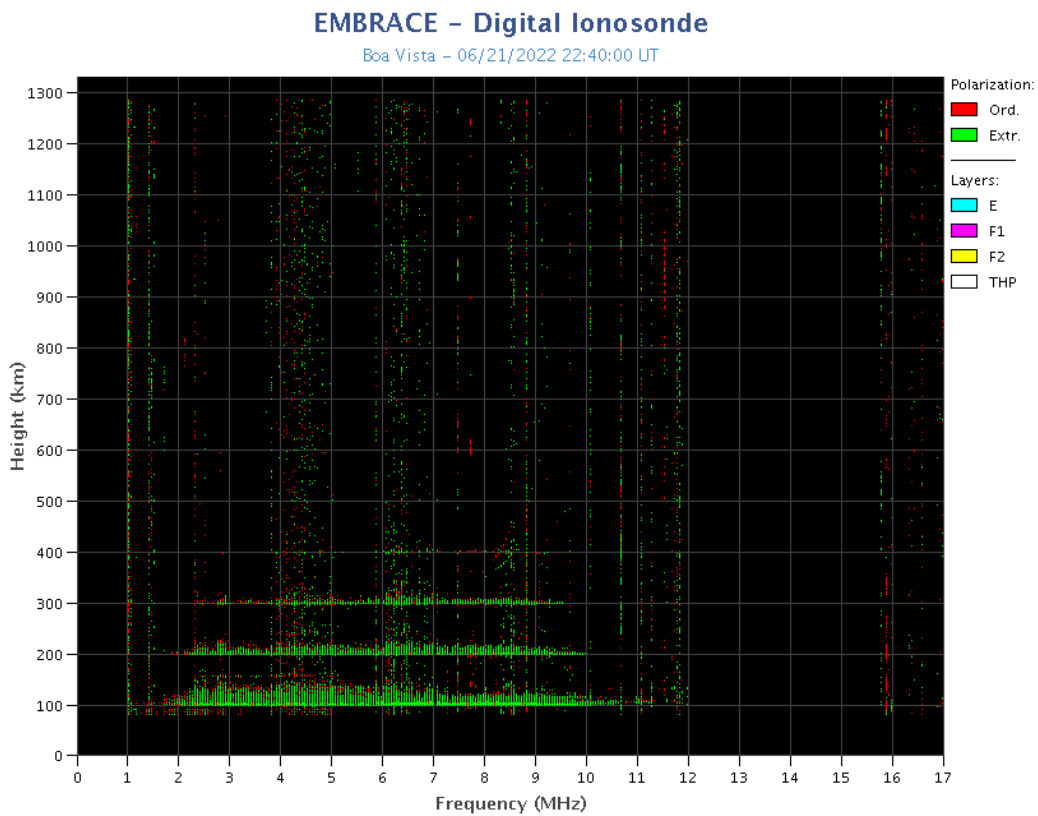
Figura 6: Time evolution of the geomagnetic Dst index.

## 8 Ionosphere

### 8.1 Responsible: Laysa Resende

#### Boa Vista:

- The spread F occurred between 21 and 25.
- The Es layers reached scale 5 on June 21.



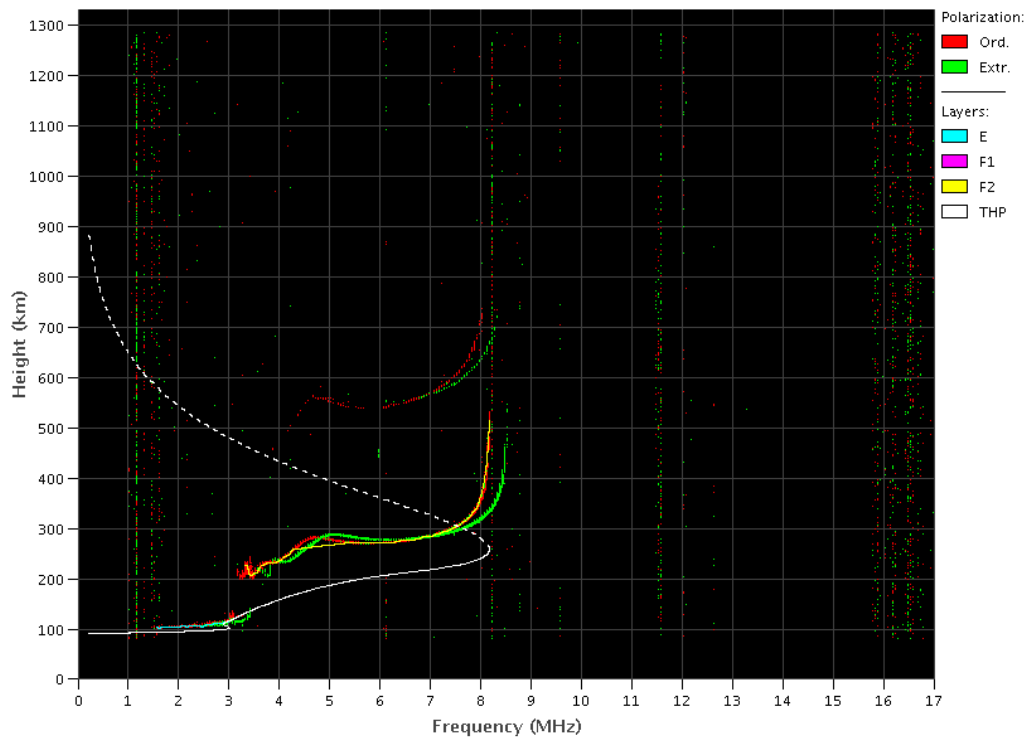
#### Cachoeira Paulista:

- The spread F did not occur during this week.
- The Es layers reached scale 3 during this week.



### EMBRACE - Digital Ionosonde

Cachoeira Paulista - 06/24/2022 12:20:00 UT



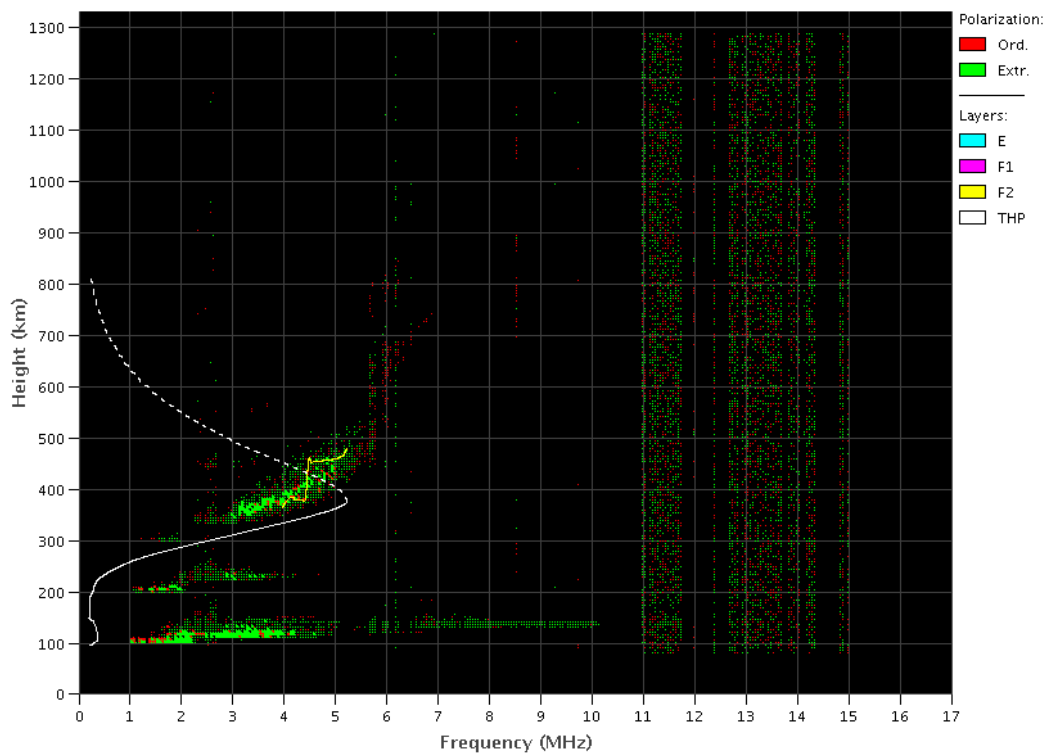
Copyright 2012 by INPE. All rights reserved.

#### São Luís:

- There were a spread F during all days in this week.
- The Es layers reached scale 4 on day 20, 21 and 23.

### EMBRACE - Digital Ionosonde

São Luís - 05/11/2022 01:40:00 UT



Copyright 2012 by INPE. All rights reserved.

## 9 Scintillation

### 9.1 Responsible: Siomel Savio Odriozola

In this report on the S4 scintillation index, data from SLMA in São Luiz/MA, STNT in Natal/RN, PALM in Palmas/TO and SJCE in São José dos Campos/SP are presented. The S4 index tracks the presence of irregularities in the ionosphere having a spatial scale  $\sim 360$  m. During this week SLMA and PALM stations showed S4 values below 0.3 throughout the week. The STNT and SJCE stations recorded moderate and strong values of scintillation respectively between the last hours of 06/25 and the first hours of 06/26 (Figure 1). In the case of a scintillation event that may be associated with the appearance of a plasma bubble out of a typical season of these events, the behavior of the interplanetary environment and the indexes of global and auroral magnetic activity, indicate as a possible cause of scintillation the penetration of disturbed ionospheric electric fields.

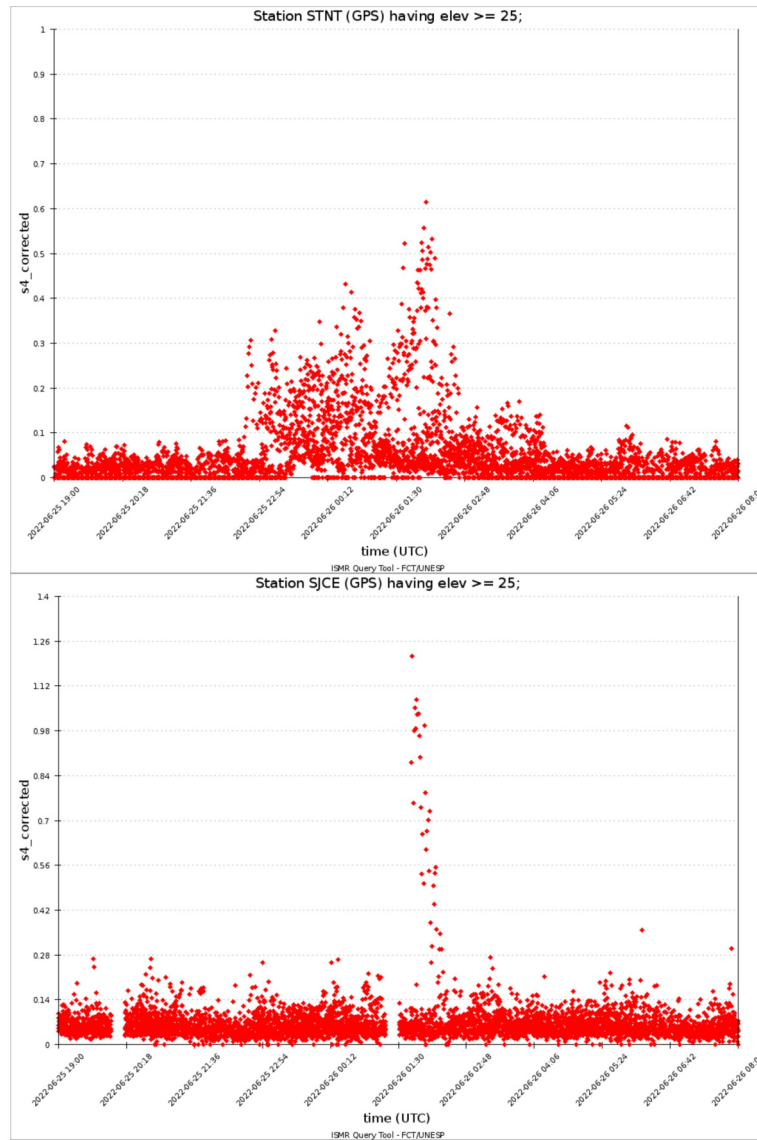


Figura 1: Valores do índice S4 para a constelação GPS medidos na estação STNT (painel superior) e SJCE (painel inferior) durante às últimas horas do dia 25/06 até as primeiras horas do dia 26/06.

## 10 All-Sky Imager

### 10.1 Responsible: LUME

**All-Sky Imager EPBs Observation**  
**Observações das EPBs por meio do imageador All-Sky**  
**June 19- June 25, 2022 || 19 de junho - 25 de junho, 2022**

| Observatory                  | June 19                              | June 20  | June 21  | June 22  | June 23  | June 24  | June 25  |
|------------------------------|--------------------------------------|----------|----------|----------|----------|----------|----------|
| Observatório                 | junho 19                             | junho 20 | junho 21 | junho 22 | junho 23 | junho 24 | junho 25 |
| CA                           | ✓○☁☁                                 | ✓☁☁☁     | ✓○☁☁     | ✓☁☁☁     | ✓☁☁☁     | ✓○☁☁     | ✓☁☁☁     |
| BJL                          | ✗                                    | ✗        | ✗        | ✗        | ✗        | ✗        | ✗        |
| CP                           | ✓○☁☁                                 | ✓○☁☁     | ✓○☁☁     | ✓○☁☁     | ✓○☁☁     | ✓○☁☁     | ✓○☁☁     |
| SMS                          | ✓○☁☁                                 | ✓○☁☁     | ✓☁☁☁     | ✓☁☁☁     | ✓☁☁☁     | ✓☁☁☁     | ✓☁☁☁     |
| <b>Definition of Symbols</b> |                                      |          |          |          |          |          |          |
| CA                           | São João do Cariri                   |          |          |          |          |          |          |
| BJL                          | Bom Jesus da Lapa                    |          |          |          |          |          |          |
| CP                           | Cachoeira Paulista                   |          |          |          |          |          |          |
| SMS                          | São Martinho da Serra                |          |          |          |          |          |          |
| ✓                            | Observation - Observação             |          |          |          |          |          |          |
| ✗                            | No Observation - Sem Observação      |          |          |          |          |          |          |
| ○                            | Clear sky - Céu limpo                |          |          |          |          |          |          |
| ☁                            | Partly Cloudy - Parcialmente Nublado |          |          |          |          |          |          |
| ☁☁                           | Cloudy - Nublado                     |          |          |          |          |          |          |

- At the Sao Joao do Cariri observatory was observed Traveling ionospheric disturbances on June 23rd and plasma bubbles on June 25th.
- At the Bom de Jesus da Lapa observatory there was no observation due to technical problems.
- At the Cachoeira Paulista observatory was observed plasma bubbles on June 25th.
- Finally, at the observatory of Sao Martinho da Serra observatory was observed plasmas bubbles on June 25th.

#### TEC

- It was observed plasma bubbles on June 25-26.